Synthesis and characterisation of the perovskite-related cuprate phases $YSr_2Cu_2MO_{7+y}$ (M=Co, Fe) for potential use as solid oxide fuel cell cathode materials

J.E.H. Sansom[1], E. Kendrick[1], H.A. Rudge-Pickard[1], M.S. Islam[1], A.J. Wright[2], and P.R. Slater[1]

[1]Chemistry, SBMS, University of Surrey, Guildford, Surrey. GU2 7XH, UK

[2]School of Chemistry, University of Birmingham, Birmingham. B15 2TT, UK

Correspondance to:

Dr. P.R. Slater

Chemistry, SBMS, University of Surrey, Guildford, Surrey. GU2 7XH. UK

Tel. +44 (0)1483 686847

Fax. +44 (0)1483 686851

e-mail: p.slater@surrey.ac.uk

Abstract

In this paper we report the synthesis and characterisation of the perovskite cuprate phases $YSr_2Cu_2MO_{7+y}$ (M=Co, Fe) to examine their potential for use as cathode materials in Solid Oxide Fuel Cells (SOFC). Both samples showed conductivities of ≈10 Scm^{-1} at 900°C and were also shown to be stable at this temperature in N_2. For $YSr_2Cu_2FeO_{7+x}$, semiconducting behaviour was observed up to ≈550°C, with a decrease in conductivity at higher temperatures, attributed to oxygen loss reducing the charge carrier concentration. In the case of $YSr_2Cu_2CoO_{7+y}$, semiconducting behaviour was observed over the range of temperatures studied, although a small but significant steep increase in conductivity was observed above 800°C. High temperature X-ray diffraction studies of this particular phase showed that this increase in conductivity coincided with an orthorhombic-tetragonal structural transition, accompanied by a significant reduction in cell volume. In addition to measurements in air, conductivities were also measured with varying $p(O_2)$ ($0.2\text{-}10^{-5}$ atm.) at 900°C, and this data showed significant hysteresis between measurements on reducing and re-oxidising, suggesting poor oxide ion transport, poor oxygen surface exchange kinetics, or significant structural changes on varying $p(O_2)$.

Chemical compatibility studies of these phases with SOFC electrolytes at temperatures between 900 and 1000°C showed reaction in all cases. In the case of CeO_2 based electrolytes, the reaction led to the formation of the "fluorite-block" phases, $(Y/Ce)_2Sr_2Cu_{3-x}M_xO_{9+y}$ (M=Co, Fe), and samples of these were subsequently prepared and the conductivities measured. Similar hysteresis between conductivity measurements on reducing and re-oxidising were also observed for these samples.

Keywords: Cuprate, perovskite, cathode, X-ray diffraction, conductivity, solid oxide fuel cell

Introduction

With the growing concerns over dwindling fuel reserves, and increasing greenhouse gas emissions, there is a steadily increasing interest in more efficient means of energy generation. One of the technologies being investigated with vigour is the fuel cell, which provides a means for directly converting chemical energy within a fuel to electrical energy. There are a number of different types of fuel cells, depending on the electrolyte employed and the temperature of operation. Solid oxide fuel cells are all solid state systems which operate at elevated temperatures (500-1000°C), and are attracting considerable interest for stationary power generation, particularly due to their potential for utilising a wide range of fuels. The current favoured materials for the electrolyte (yttria stablised zirconia, YSZ), the anode (a Ni/YSZ cermet) and the cathode ($La_{1-x}Sr_xMnO_3$) all have some operating problems. In the case of the cathode, $La_{1-x}Sr_xMnO_3$ shows low levels of oxide ion conductivity, hence although O_2 can be reduced to O^{2-} at the surface of the cathode, these oxide ions cannot easily migrate through the cathode to the electrolyte. Hence the surface area of reaction is essentially limited to the three phase boundaries between the cathode, electrolyte, and oxygen gas. It is with a view to solving some of these problems that our research has concentrated on alternative materials, and in this paper we present an investigation of some cuprate phases related to high temperature superconducting systems for possible use as SOFC cathodes.

Prior research in this area by Fletcher *et al.* has investigated the use of $YBa_2Cu_3O_{7-y}$, a superconductor below 93K, as a possible cathode material for SOFCs [1]. However, the results showed that the material experienced a number of problems. At raised temperatures (>900^{o}C) there was significant degradation of the structure including

decomposition and a reaction with YSZ. There was also electrochemical decomposition at fairly low current densities (20 $mAcm^{-2}$) [1]. This compound has two copper sites, one site (Cu2) associated with the superconducting CuO_2 layers, and a second site (Cu1) which links these layers along the c direction (figure 1). The main stability problem is located at the Cu1 site. In the fully oxidised material, $y \approx 0$, this Cu atom is in square planar coordination. If the material is reduced at high temperatures in an inert atmosphere (such as Ar or N_2) oxygen is lost reducing this Cu to Cu^{1+} with linear coordination. Further reduction at higher temperatures leads then to decomposition of the sample. In order to minimise or remove this instability, the Cu at the Cu1 site can be either partially or completely replaced by other cations, ranging from Al, Ga, to transition metals, and even oxyanions (SO_4^{2-}, BO_3^{3-}). Co-substitution of Sr for Ba has the effect of improving the thermal stability. Phases of the form $YSr_2Cu_{3-x}M_xO_{7-y}$ (M=Ga, Al, Co, Fe, S, P, B) [2-9] can thus be prepared, two examples being $YSr_2Cu_2CoO_{7+y}$ and $YSr_2Cu_2FeO_{7+y}$. Previous structural work on the Fe containing system, $YSr_2Cu_2FeO_{7+y}$, has shown that although Fe exhibits a preference for substitution onto the Cu1 site, this is not complete and a small amount of Fe does enter the Cu2 site. In addition this material also contains oxygen excess, $y \approx 0.4$-0.5, as prepared, with this "excess" oxygen going into normally unoccupied positions around the Fe in the Cu1 sites, raising the coordination for some of the Fe atoms from 4 to 5/6 coordination (figure 2) [3]. Recent reports have suggested that annealing at high temperature under N_2 can lead to a redistribution of Fe, so that all the Fe occupies the Cu1 site [10]. Such samples are then superconducting after subsequent low temperature oxidation.

In the case of $YSr_2Cu_2CoO_{7+y}$ previous structural studies have shown that y≈0, and all the Co is located on the Cu1 site with tetrahedral coordination, leading to cooperative oxygen ordering and an expanded √2a x √2b x 2c cell (figure 3) [4,5].

Although these phases have been known for several years, studies of their high temperature conductivity have been lacking. In a previous paper, we reported preliminary conductivity studies of these phases [11], and in this paper we expand this work with detailed studies of the evolution of their structures and conductivities with temperature and $p(O_2)$, in order to evaluate their potential as SOFC cathode materials.

In addition to measuring the conductivity characteristics of these materials, chemical compatibility of these phases with SOFC electrolyte materials has also been investigated. Following results of these compatibility studies, the conductivities of the "fluorite- block" phases $Y_{1.5}Ce_{0.5}Sr_2Cu_{2.5}M_{0.5}O_{9+y}$ (M=Co, Fe) have also been investigated and are reported here.

Experimental

High purity Y_2O_3, $SrCO_3$, CuO, Fe_2O_3, Co_3O_4 were used to prepare the samples $YSr_2Cu_2MO_{7+y}$ (M=Co, Fe). The starting materials were ground in the stoichiometric ratios and heated to 1000°C for 16 hours. The powders were then reground and reheated under the same conditions. Sample purity was examined using X-ray diffraction (Seifert XRD3003TT diffractometer). High temperature X-ray diffraction data were collected on a Siemens D5005 diffractometer with an Anton Parr HTK 1200 heating stage.

Thermal expansion measurements were performed using a Linseis L76 dilatometer (heating rate 5°C/min to 900°C)

Oxygen contents were determined by thermogravimetric analysis (reduction ($5\%H_2/95\%N_2$) at 950°C) using a Stanton Redcroft STA 780 thermal analyser. The method was also used to investigate oxygen loss within the samples on heating between 25 and 900°C (heating rate 10°C/min, held at 900°C for 20 min) in both air and N_2.

Conductivity measurements were made using the standard four probe d.c. technique. Sintered pellets were prepared by pressing at 6000 kg cm^{-2} and sintering at 1000°C for 16 hours. Densities of 80-84% of the theoretical were obtained using these conditions. Conductivity measurements were then taken in air as a function of temperature (25-900°C). Measurements of the conductivity versus oxygen partial pressure (measured via a YSZ sensor) were made at a temperature of 900°C. For these measurements, the conductivities were initially taken in moving from oxidising to reducing conditions, where nitrogen was allowed to pass into the system. In this case the change in $p(O_2)$ proceeds quite rapidly ($0.2\text{-}10^{-5}$ atm. in about 1 hour). The sample was then held under a N_2 atmosphere for at least 15 hours, in order for the system under test to reach equilibration, prior to any measurements being taken in the reverse direction (from reducing to oxidising). The N_2 flow was then turned off, and oxygen was allowed to leak back into the system naturally. This typically took a period of approximately 24 hours, with measurements made over this time. Sample purity before and after measurement was confirmed using X-ray diffraction.

The chemical compatability of the phases $YSr_2Cu_2MO_{7+y}$ (M=Co, Fe) with potential solid oxide fuel cell electrolytes was examined by grinding together the sample and electrolyte

in a 1:1 by mass ratio and heating at temperatures between 900 and 1000°C for 1-3 weeks. A range of potential solid oxide fuel cell electrolytes were examined to include yttria stabilised zirconia $Y_{0.15}Zr_{0.85}O_{1.925}$ (YSZ), gadolinia doped ceria $Gd_{0.1}Ce_{0.9}O_{1.95}$ (CGO), $La_{0.9}Sr_{0.1}Ga_{0.8}Mg_{0.2}O_{2.85}$, and Apatite-type $La_{9.33}(Si/Ge)_6O_{26}$.

Results and Discussion

X-ray diffraction showed the successful synthesis of single phase samples of both $YSr_2Cu_2FeO_{7+y}$ and $YSr_2Cu_2CoO_{7+y}$. The oxygen contents determined from TGA studies were 7.42(4) for $YSr_2Cu_2FeO_{7+y}$ and 7.03(4) for $YSr_2Cu_2CoO_{7+y}$ consistent with previous studies of these phases [3-5]. In the case of $YSr_2Cu_2CoO_{7+y}$, no measureable oxygen loss was observed in air or N_2 between 25 and 900ºC. In contrast, $YSr_2Cu_2FeO_{7+y}$ showed significant oxygen loss, with the oxygen content in air decreasing to 7.19(4) at 900ºC, while heating in N_2 resulted in a greater mass loss to 7.03(4) at 900ºC.

Conductivity studies

The conductivities of both samples showed a decrease with decreasing oxygen partial pressure, indicating that these materials are p-type conductors. The data showed significant hysteresis between measurements on reducing and then re-oxidising (figure 4). This hysteresis suggests slow equilibration between the sample and the atmosphere, which is indicative of poor oxide ion transport, poor oxygen surface exchange kinetics, or significant structural changes on varying $p(O_2)$.

The poor equilibration meant that it was not possible to calculate accurate gradients for the plots of log σ vs log $p(O_2)$ to relate to defect equations. Attempts were made to prepare more porous pellets by sintering at lower temperatures (900ºC) in order to improve the equilibration, however such samples proved to be very brittle in nature, making measurement very difficult.

Although the poor equilibration meant that detailed conductivity versus $p(O_2)$ data could not be interpreted, an average gradient could, however, be determined from the two end points (0.2, $\approx 10^{-5}$ atm.) of the graph, since at these two data points the samples were well equilibrated. From these points, it was clear that the $p(O_2)$ dependence of the conductivity of $YSr_2Cu_2FeO_{7+x}$ was much greater than that of $YSr_2Cu_2CoO_{7+y}$, with approximate gradients of 0.37 and 0.08 respectively. The origin of this increased $p(O_2)$ dependence could be related to two factors. Firstly TGA data indicates that there is a large change in oxygen stoichiometry in $YSr_2Cu_2FeO_{7+y}$ on changing from air to N_2, with oxygen contents of 7.19(4) and 7.03(4) in air and N_2 respectively at 900ºC. This significant decrease in oxygen content would lead to a significant decrease in the number of charge carriers, and corresponding decrease in conductivity. In contrast negligible change in oxygen content was observed for $YSr_2Cu_2CoO_{7+y}$. A second factor influencing the $p(O_2)$ dependance could be a redistribution of Fe over the two Cu sites under N_2, with an increase in Fe occupancy of the Cu1 site and consequent decrease in the occupancy at the Cu2 site, as suggested previously in the literature [10]. If redistribution of Fe over the two Cu sites is occurring under the experimental conditions employed, then this could also help to explain the large hysteresis observed between conductivity data on reducing and re-oxidising, since such a redistribution of Fe is likely to be a slow process.

The variation of the conductivity with temperature in air was also examined for both samples. This data showed some interesting variations (figure 5). Firstly the conductivity of $YSr_2Cu_2FeO_{7+y}$ shows semiconducting behaviour up to ≈550°C, before a gradual decrease in conductivity is observed as the temperature is raised ($\sigma_{550°C}$= 35 Scm^{-1}, $\sigma_{900°C}$= 6 Scm^{-1}). This decrease in conductivity at higher temperatures can be related to oxygen loss reducing the number of charge carriers (from TGA studies, the oxygen contents in air at 25ºC and 900ºC are 7.42(4) and 7.19(4) respectively). The oxygen excess and consequent variable valency for $YSr_2Cu_2FeO_{7+y}$ explains why the room temperature conductivity is significantly higher than for the nominally oxygen stoichiometric $YSr_2Cu_2CoO_{7+y}$.

In order to investigate the evolution of structure with temperature, X-ray diffraction data were collected up to 950ºC, and cell parameters were refined (figure 6). The data showed no change in cell symmetry over the range of temperatures employed, with the cell being tetragonal over the full range. However, it is clear from the data that the variation of cell parameters with temperature is non-linear, especially for the a,b parameters, which can be attributed to the observed oxygen loss on heating to high temperature. This non-linear thermal expansion was also shown from dilatometry studies (figure 7), with the thermal expansion coefficient increasing from 13.0 x 10^{-6} K^{-1} to 17.3 x 10^{-6} K^{-1} between 400 and 900ºC. The thermal expansion coefficient at high temperatures is significantly higher than those of fuel cell electrolyte materials such as YSZ (≈10.5 x 10^{-6} K^{-1}), which represents an additional problem with employing this material in SOFC applications.

In the case of $YSr_2Cu_2CoO_{7+y}$, the variation in conductivity with temperature was particularly interesting. Here the sample showed semiconducting behaviour for the whole

temperature range examined. However, a small but significant step increase in the conductivity was observed above 800°C. In order to investigate this further, high temperature XRD data were collected as for $YSr_2Cu_2FeO_{7+y}$, and cell parameters refined (figure 8). Whereas there was no change in cell symmetry from 25-950ºC for $YSr_2Cu_2FeO_{7+y}$, the data for $YSr_2Cu_2CoO_{7+y}$ showed a clear change in symmetry from orthorhombic to tetragonal at high temperature. The transition occurs at a similar temperature to that observed for the increase in conductivity from the conductivity data. Accompanying the transition is a significant reduction in the c axis length, and overall reduction in cell volume. The unit cell contraction at the phase transition was confirmed from dilatometry (figure 9). Above the phase transition the thermal expansion coefficient was $\approx 13.0 \times 10^{-6}\ K^{-1}$, while below it is $\approx 12.3 \times 10^{-6}\ K^{-1}$. These values are closer to that of YSZ than for $YSr_2Cu_2FeO_{7+x}$, although the phase change and accompanying volume contraction would potentially cause problems in applications as SOFC cathodes, e.g. it may result in delamination of the cathode layer.

As regards the effect of this structural transition on the conductivity, it is possible that the significant contraction along c could be accompanied by a redistribution of charge between the Cu and Co sites. Such a redistribution of charge could then account for the observed small but significant step increase in conductivity. Further detailed studies by neutron diffraction are required to investigate this transition in more detail.

Chemical compatibility studies

Chemical compatibility studies were performed between these samples and potential SOFC electrolytes, since in SOFC operation, any reaction may lead to potential problems at the interface between the electrolyte and electrode. Initial studies were carried out at 900ºC, and these were then repeated at a temperature of 1000ºC. In all cases, the studies showed significant reaction, which would be likely to cause problems in the use of these materials as SOFC cathodes. In the case of YSZ, reaction gave rise to the formation of $SrZrO_3$ impurity after heating for a period of 1 week at 900ºC. Since $SrZrO_3$ is electrically insulating, the formation of this phase at the interface between electrolyte and cathode would present a major problem. It therefore seems as if these materials are not suitable for use with YSZ electrolytes at high temperatures (900ºC or above). It may be possible to use these materials with YSZ electrolytes at lower temperatures, although heating for a short time at elevated temperatures is likely to be required to ensure bonding to the electrolyte.

In the case of the perovskite-type electrolyte $La_{0.9}Sr_{0.1}Ga_{0.8}Mg_{0.2}O_{2.85}$, there was no obvious reaction with the cuprate materials after heating for 1 week at 900ºC. Significant reaction was only observed when the mixtures were heated for two weeks at 1000ºC. Under such conditions, the XRD data suggested the formation of mixed perovskite phase impurities, $(La/Sr)(Cu/M)O_{3-y}$ (M=Co, Fe, Ga), and $Y_2Cu_2O_5$.

Impurity phases were also formed on heating the cuprate phases with apatite-type materials, $La_{9.33}(Si/Ge)_6O_{26}$. In these cases heating at 1000ºC suggested the formation of $(La/Sr)_2CuO_{4-y}$, as well as other unidentified phases. In addition, the XRD peaks for the apatite electrolyte were shown to shift slightly to lower angles, suggesting incorporation of Co, Fe into the apatite structure. Previous studies of apatite electrolytes have shown

that Fe and Co can substitute onto the Si site in such phases leading to an expansion of the unit cell [12, 13].

In the case of CeO_2 based electrolytes (CGO), there was no obvious reaction at 900ºC, although at higher temperatures, 1000ºC, reaction gave rise to the formation of the "fluorite block" phases $(Y/Ce)_2Sr_2Cu_{3-x}M_xO_{9+y}$ (M=Co, Fe). As these phases are likely to be conducting, this reaction with CeO_2 based electrolytes may be less of a problem compared to the products formed with the other electrolytes examined. In order to confirm the conducting nature of these phases, the preparation of two samples $Y_{1.5}Ce_{0.5}Sr_2Cu_2FeO_{9+y}$ and $Y_{1.5}Ce_{0.5}Sr_2Cu_2CoO_{9+y}$ was attempted, although initial attempts to prepare such phases resulted in small impurities. As a result, phases with lower Co, Fe content, $(Y/Ce)_2Sr_2Cu_{2.5}M_{0.5}O_{9+y}$ (M=Co, Fe), were prepared, and were shown to be single phase, with cell parameters of a=b=3.823(2), c=28.34(2) Å (M=Co) and a=b=3.813(5), c=28.40(3) Å (M=Fe). The conductivities of these samples were then examined with varying temperature and $p(O_2)$.

These conductivity data are shown in figures 10 and 11. The low temperature conductivities were significantly higher than observed for either $YSr_2Cu_2CoO_{7+y}$ or $YSr_2Cu_2FeO_{7+y}$ (figure 9). This can be explained by the replacement of Y^{3+} by a $(Y_{1.5}Ce_{0.5}O_2)^{2.5+}$ unit, the lower charge for the latter giving rise to oxidation of the CuO_2 planes and an increase in conductivity. As for the $YSr_2Cu_2MO_{7+y}$ samples, significant hysteresis between conductivity data on reducing and re-oxidising was observed (figure 11). In addition both samples showed a large average gradient of conductivity versus $p(O_2)$, 0.33 for M=Co, and 0.44 for M=Fe. Further high temperature studies are required to look into these features in more detail. Nevertheless the high conductivities observed

for these phases may suggest that the reactivity between $YSr_2Cu_2MO_{7+y}$ and CeO_2 based electrolytes is not as large a problem as for the other electrolytes.

Conclusions

In conclusion the cuprate systems, $YSr_2Cu_2MO_{7+y}$ (M=Co, Fe), have been investigated as possible cathode materials for SOFCs, with the data suggesting significant problems with these materials for such applications. The examination of the conductivity with varying $p(O_2)$ shows significant hysteresis between the data obtained on reducing and that obtained on re-oxidising. This suggests that the samples show slow oxygen transport/surface exchange or significant structural changes on varying $p(O_2)$. In addition to the observed hysteresis, the samples show significant reactivity with a range of SOFC electrolyte materials at elevated temperatures. However, in some cases (e.g. CeO_2 based electrolytes) the reaction products showed good conductivities, which may indicate this to be less of a problem.

The variation of conductivities with temperature showed some interesting features, in particular for $YSr_2Cu_2CoO_{7+y}$, for which an increase in conductivity above 800ºC was attributed to an orthorhombic-tetragonal phase transition, accompanied by a reduction in cell volume.

Acknowledgements

We would like to thank EPSRC and Merck Ltd for funding

References

1. J.G. Fletcher, J.T.S. Irvine, A.R. West, J.A. Labrinca, J.R. Frade, F.M.B. Marques; *Mater. Res. Bull.* **29** (1994) 1175.
2. P.R. Slater and C. Greaves; *Physica C* **180** (1991) 299.
3. T. Den and T. Kobayashi; *Physica C* **196** (1992) 141.
4. G. Roth, P. Adelmann, G. Heger, R. Knitter, T. Wolf; *J. Phys.* **1** (1991) 721.
5. S.A. Sunshine, L.F. Schneemeyer, T. Siegrist, D.C. Douglas, J.V. Waszczak, R.J. Cava, E.M. Gyorgy, D.W. Murphy; *Chem. Mater.* **1** (1989) 331.
6. L.E. Moran, R. Rojas, M.A. Alario-Franco; *J. Mater. Chem.* **6** (1996) 1517.
7. P.R. Slater and C. Greaves; *Physica C* **215** (1993) 191.
8. P.R. Slater, C. Greaves, M. Slaski, C.M. Muirhead; *Physica C* **208** (1993) 193.
9. J.Q. Li, W.J. Zhu, Z.X. Zhao, D.L. Yin; *Solid State Commun.* **85** (1993) 739.
10. J. Shimoyama, K. Otzschi, T. Himouchi, K. Kishio, *Physica* C **341** (2000) 563.
11. J.E.H. Sansom, H.A. Rudge-Pickard, G. Smith, P.R. Slater, M.S. Islam; *Solid State Ionics* **175** (2004) 99.
12. J. McFarlane, S. Barth, M. Swaffer, J.E.H. Sansom, P.R. Slater, *Ionics* **8** (2002) 149.
13. A.L. Shaula, V.V. Kharton, M.V. Patrakeev, J.C. Waerenborgh, D.P. Rojas, N.P. Vyshatko, E.V. Tsipis, A.A. Yaremchenko, F.M.B. Marques; *Mater. Res. Bull.* **39**, (2004) 763.

Figure captions

Figure 1. The structure of $YBa_2Cu_3O_{7-x}$

Figure 2. The structure of $YSr_2Cu_2FeO_{7+y}$

Figure 3. The structure of $YSr_2Cu_2CoO_7$

Figure 4. Plot of log σ vs log $p(O_2)$ at 900°C for (a) $YSr_2Cu_2CoO_{7+y}$, (b) $YSr_2Cu_2FeO_{7+y}$

Figure 5. Plot of log σ vs 1/T for (a) $YSr_2Cu_2FeO_{7+y}$, (b) $YSr_2Cu_2CoO_{7+y}$

Figure 6a. Plot of cell parameters vs temperature for $YSr_2Cu_2FeO_{7+y}$

Figure 6b. Plot of cell volume vs temperature for $YSr_2Cu_2FeO_{7+y}$ (connecting lines drawn as a guide to the eye).

Figure 7. Plot of thermal expansion of $YSr_2Cu_2FeO_{7+y}$

Figure 8a. Plot of cell parameters vs temperature for $YSr_2Cu_2CoO_{7+y}$

Figure 8b. Plot of cell volume vs temperature for $YSr_2Cu_2CoO_{7+y}$

Figure 9. Plot of thermal expansion of $YSr_2Cu_2CoO_{7+y}$

Figure 10. Plot of log σ vs log $p(O_2)$ at 900°C for (a) $Y_{1.5}Ce_{0.5}Sr_2Cu_{2.5}Co_{0.5}O_{9+y}$, (b) $Y_{1.5}Ce_{0.5}Sr_2Cu_{2.5}Fe_{0.5}O_{9+y}$

Figure 11. Plot of log σ vs 1/T for (a) $Y_{1.5}Ce_{0.5}Sr_2Cu_{2.5}Co_{0.5}O_{9+y}$, (b) $Y_{1.5}Ce_{0.5}Sr_2Cu_{2.5}Fe_{0.5}O_{9+y}$

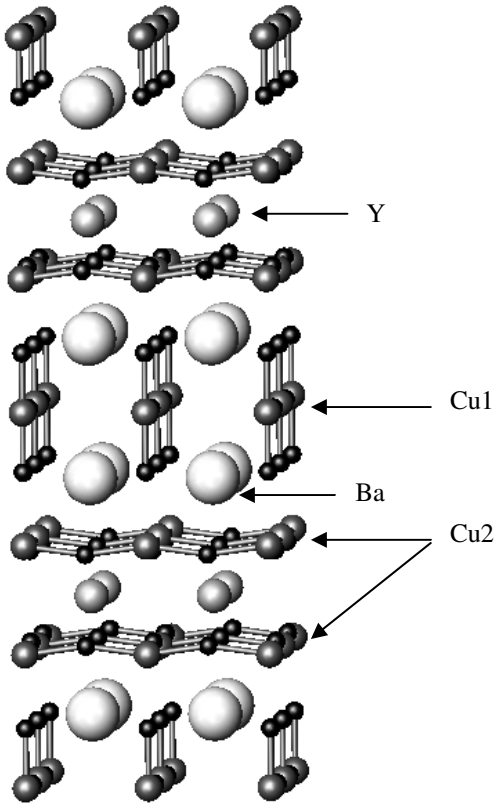

Figure 1. The structure of $YBa_2Cu_3O_{7-x}$

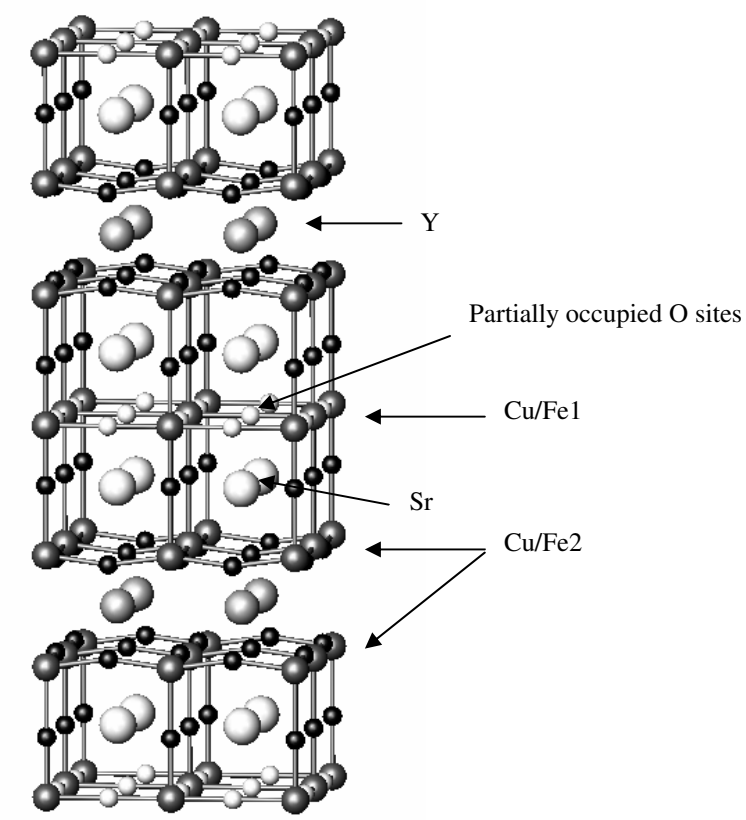

Figure 2. The structure of $YSr_2Cu_2FeO_{7+y}$

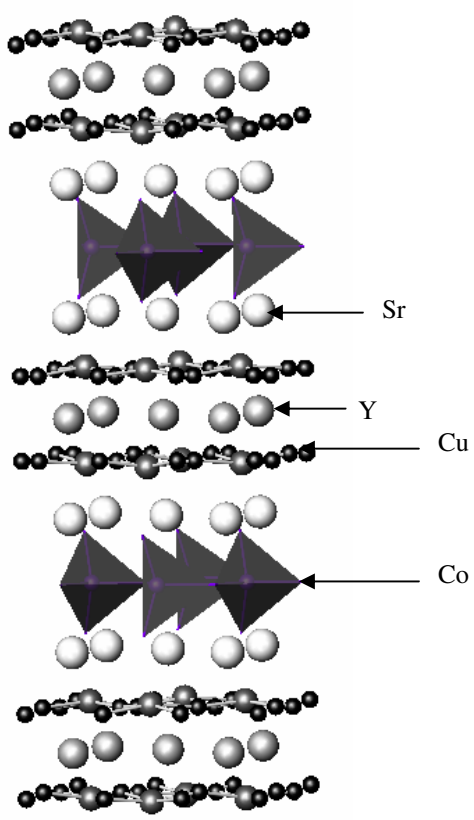

Figure 3. The structure of $YSr_2Cu_2CoO_7$

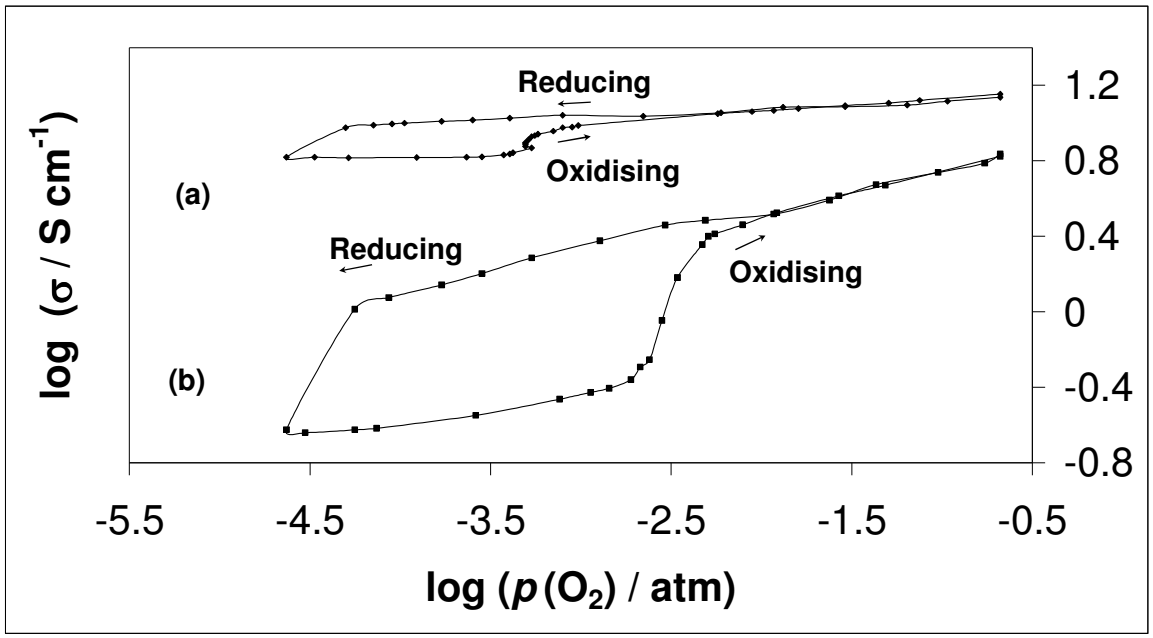

Figure 4. Plot of log σ vs log p(O_2) at 900°C for (a) $YSr_2Cu_2CoO_{7+y}$, (b) $YSr_2Cu_2FeO_{7+y}$

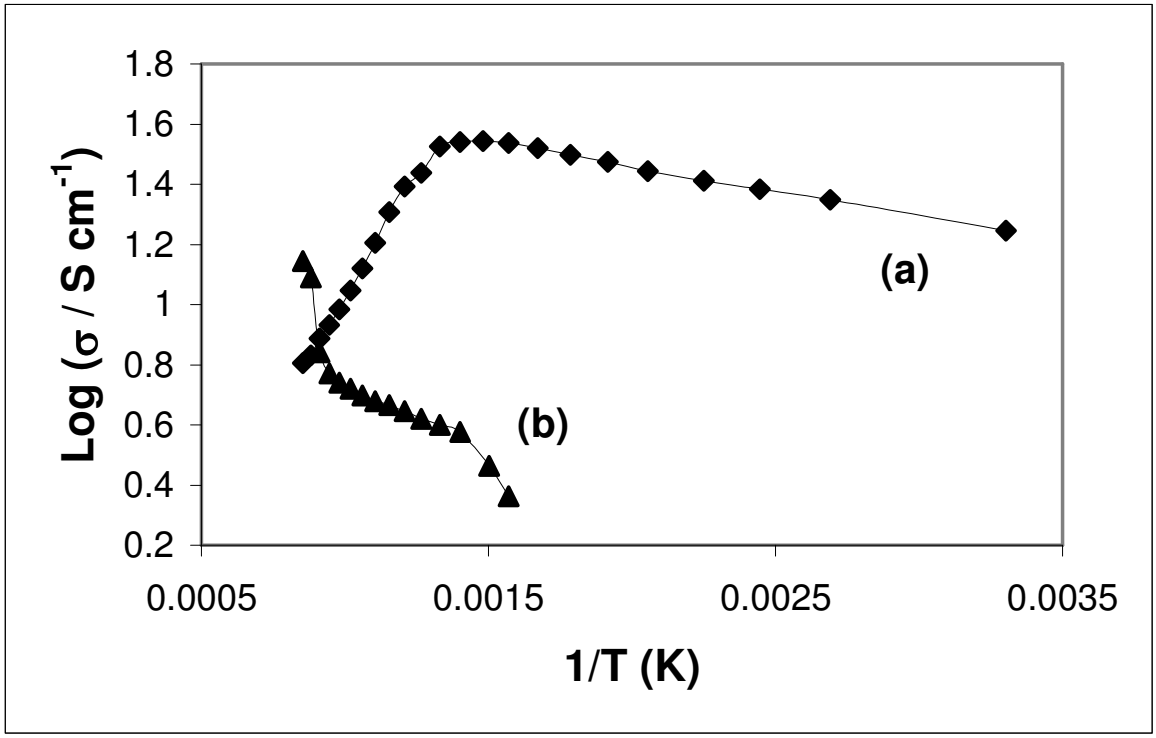

Figure 5. Plot of log σ vs 1/T for (a) $YSr_2Cu_2FeO_{7+y}$, (b) $YSr_2Cu_2CoO_{7+y}$

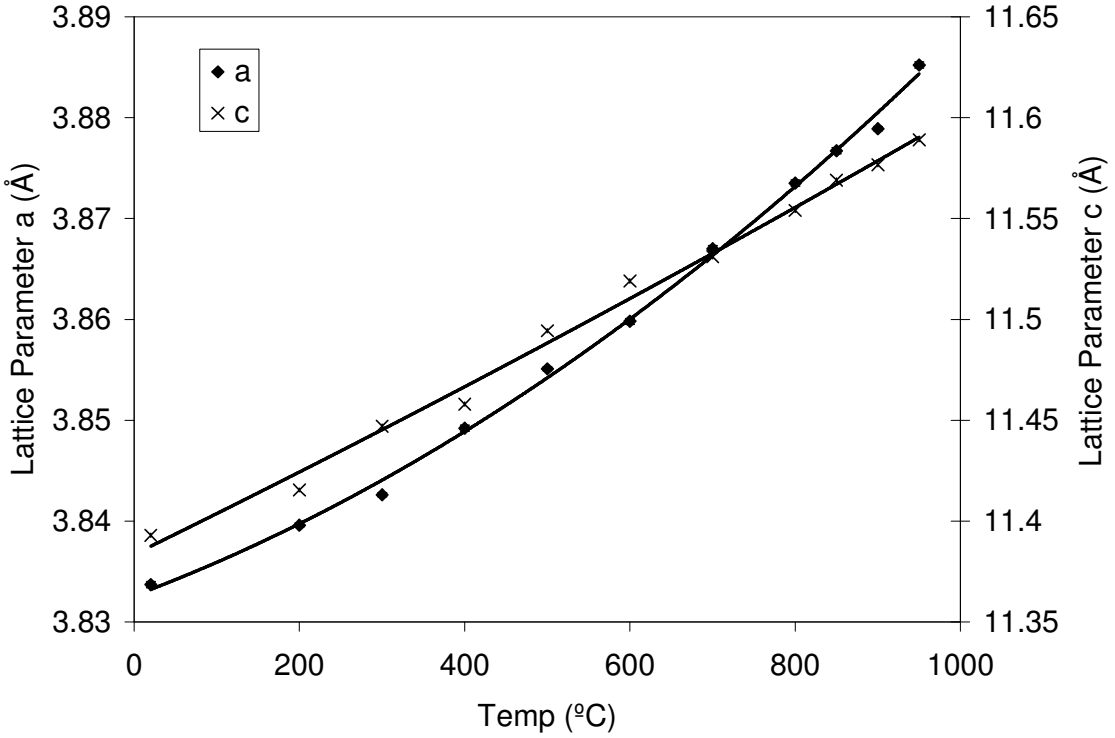

Figure 6a. Plot of cell parameters vs temperature for $YSr_2Cu_2FeO_{7+y}$

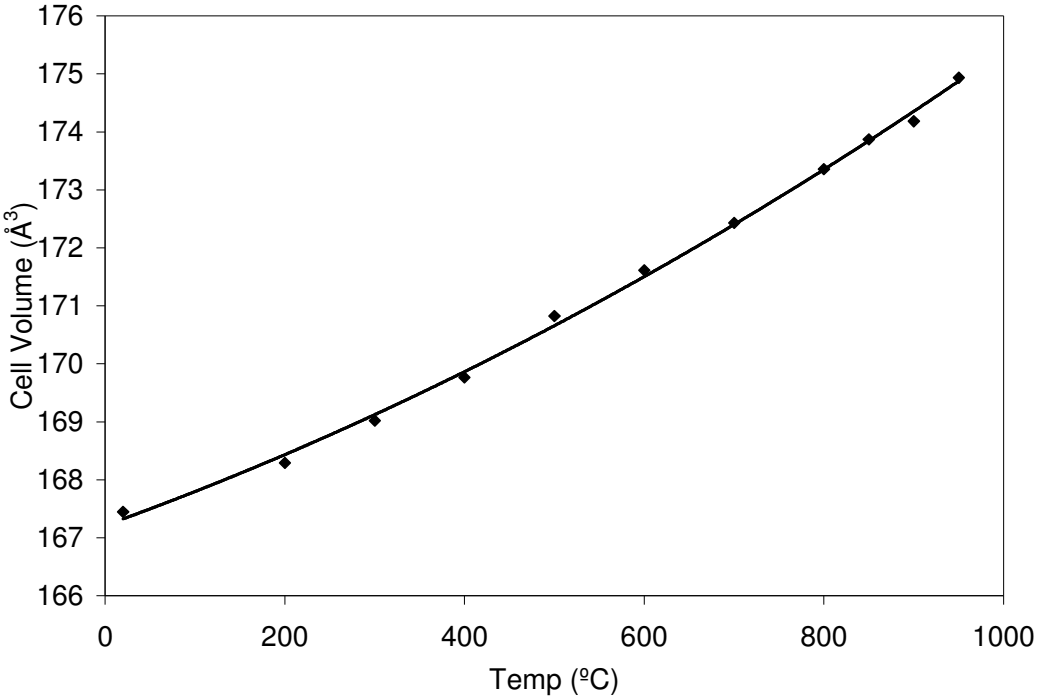

Figure 6b. Plot of cell volume vs temperature for $YSr_2Cu_2FeO_{7+y}$

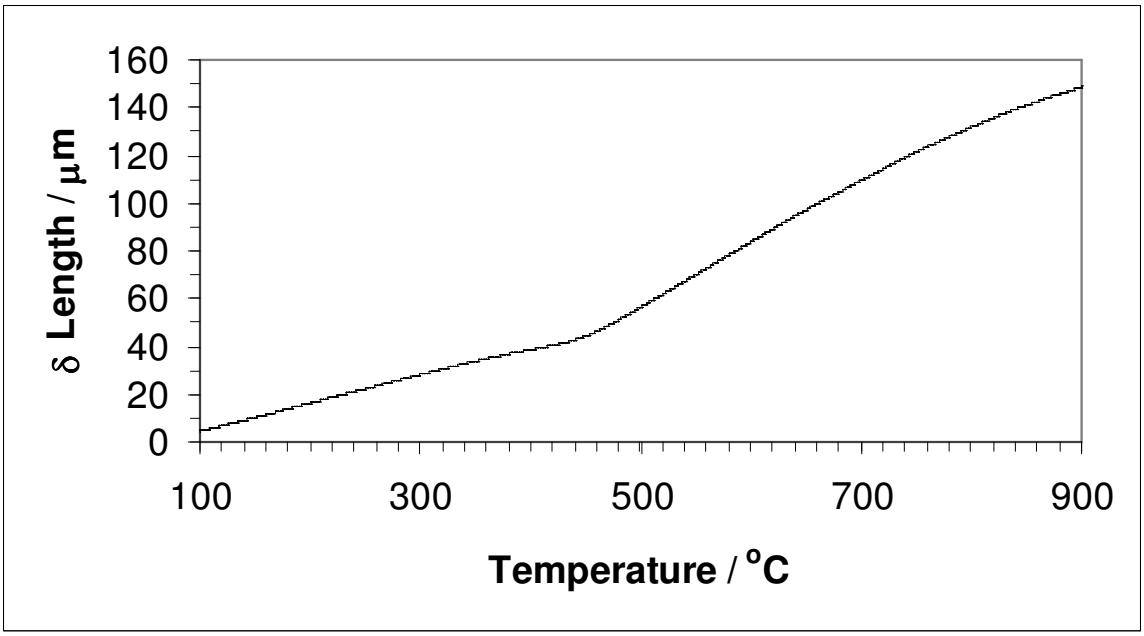

Figure 7. Plot of thermal expansion of $YSr_2Cu_2FeO_{7+y}$

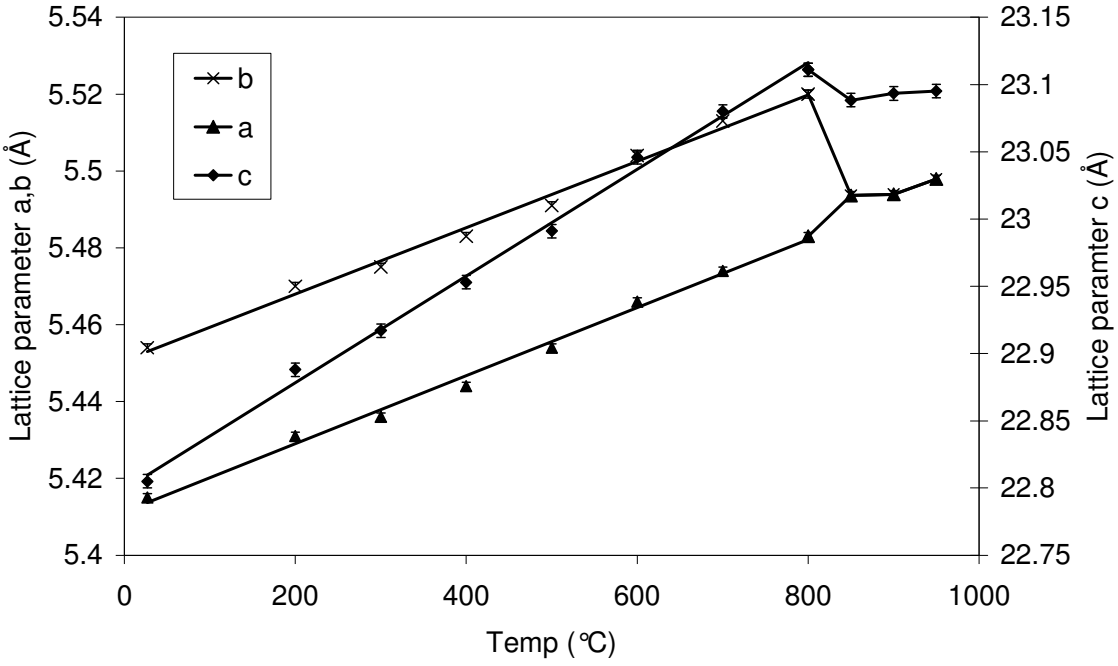

Figure 8a. Plot of cell parameters vs temperature for $YSr_2Cu_2CoO_{7+y}$

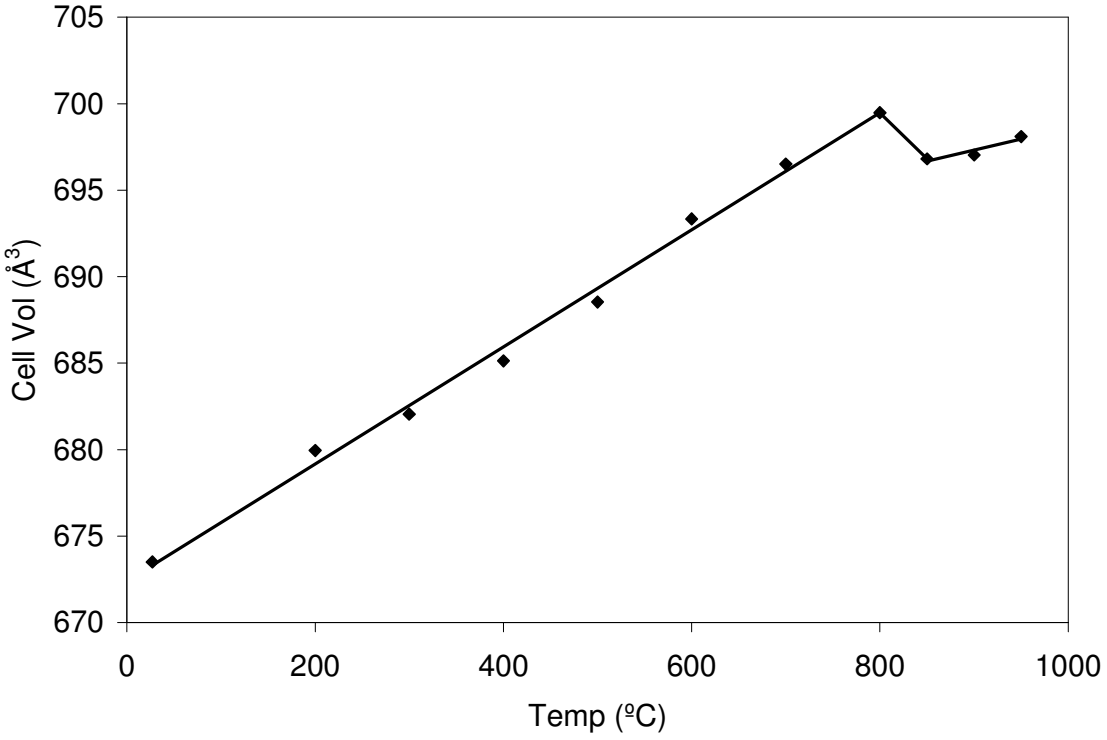

Figure 8b. Plot of cell volume vs temperature for $YSr_2Cu_2CoO_{7+y}$

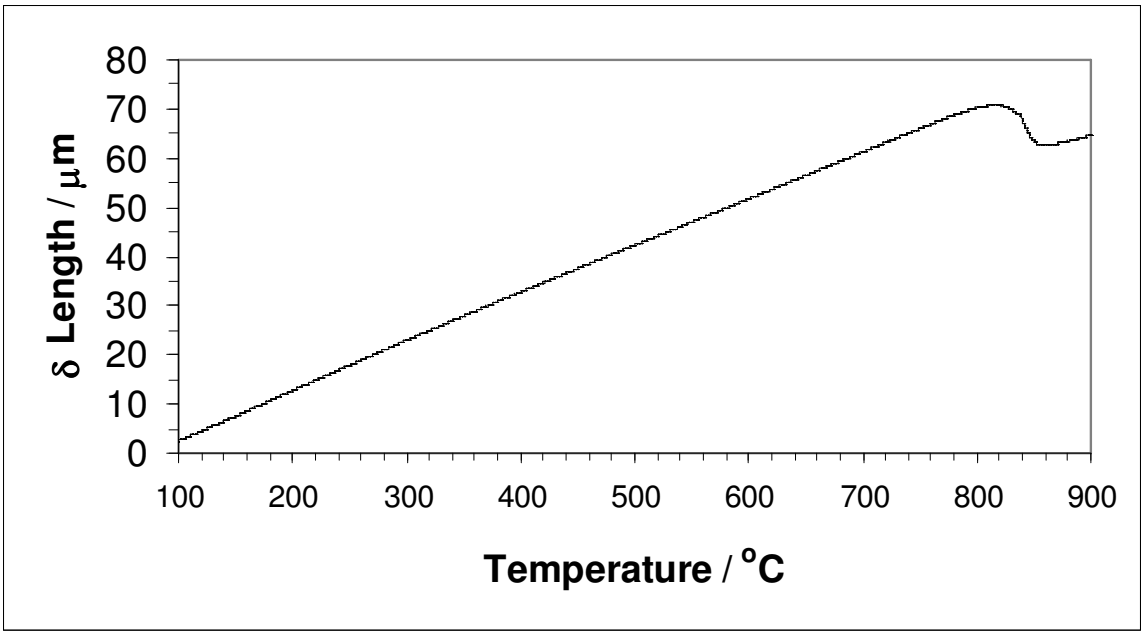

Figure 9. Plot of thermal expansion of $YSr_2Cu_2CoO_{7+y}$

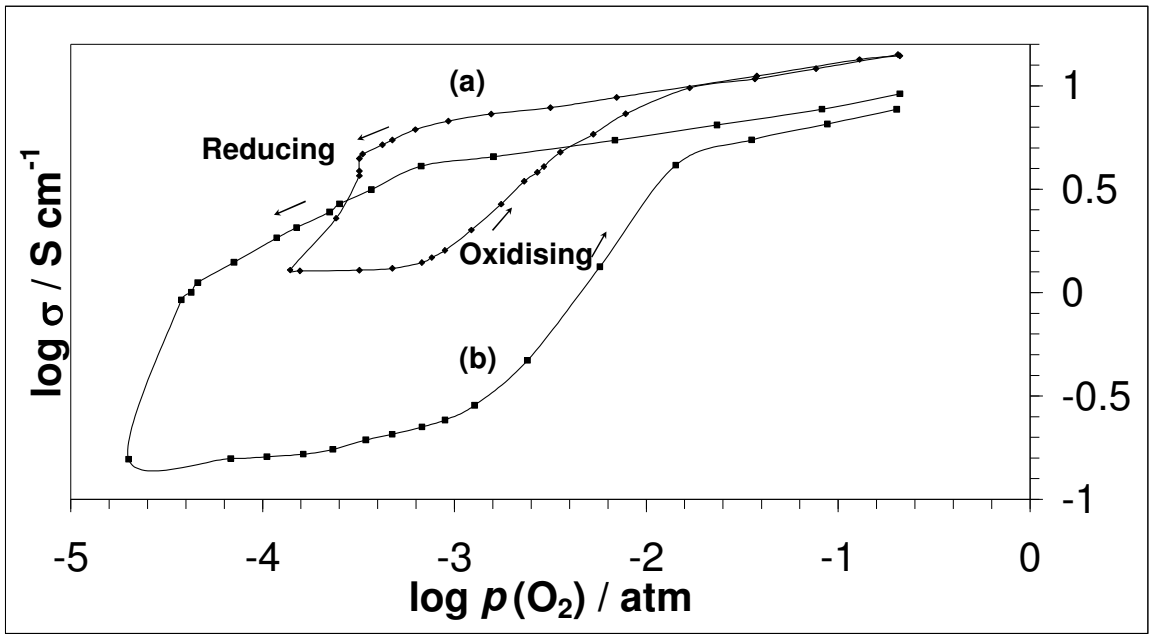

Figure 10. Plot of log σ vs log p(O_2) at 900°C for (a) $Y_{1.5}Ce_{0.5}Sr_2Cu_{2.5}Co_{0.5}O_{9+y}$, (b) $Y_{1.5}Ce_{0.5}Sr_2Cu_{2.5}Fe_{0.5}O_{9+y}$

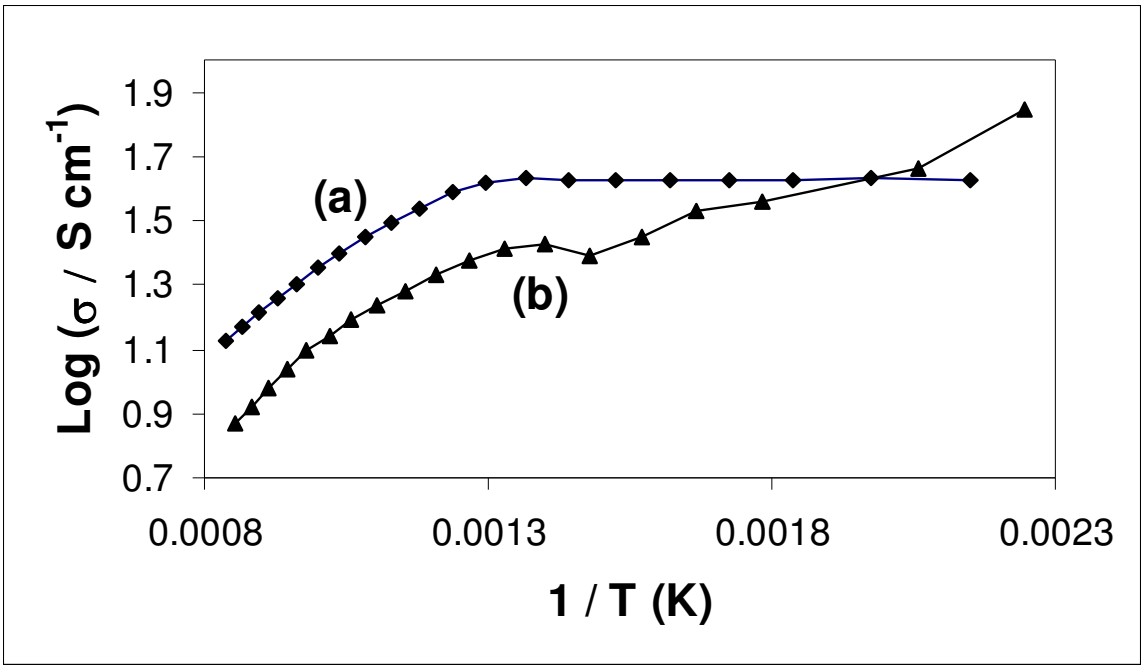

Figure 11. Plot of log σ vs 1/T for (a) $Y_{1.5}Ce_{0.5}Sr_2Cu_{2.5}Co_{0.5}O_{9+y}$, (b) $Y_{1.5}Ce_{0.5}Sr_2Cu_{2.5}Fe_{0.5}O_{9+y}$